ORIGINAL ARTICLE

Reduction of *Ptf1a* Gene Dosage Causes Pancreatic Hypoplasia and Diabetes in Mice

Akihisa Fukuda,[1,2,3] Yoshiya Kawaguchi,[1] Kenichiro Furuyama,[1] Sota Kodama,[1] Masashi Horiguchi,[1] Takeshi Kuhara,[1] Michiya Kawaguchi,[1] Mami Terao,[4] Ryuichiro Doi,[1] Christopher V.E. Wright,[5] Mikio Hoshino,[4,6] Tsutomu Chiba,[2] and Shinji Uemoto[1]

OBJECTIVE—Most pancreatic endocrine cells derive from *Ptf1a*-expressing progenitor cells. In humans, nonsense mutations in *Ptf1a* have recently been identified as a cause of permanent neonatal diabetes associated with pancreatic agenesis. The death of *Ptf1a*-null mice soon after birth has not allowed further insight into the pathogenesis of the disease; it is therefore unclear how much pancreatic endocrine function is dependent on *Ptf1a* in mammals. This study aims to investigate gene-dosage effects of *Ptf1a* on pancreas development and function in mice.

RESEARCH DESIGN AND METHODS—Combining hypomorphic and null alleles of *Ptf1a* and Cre-mediated lineage tracing, we followed the cell fate of reduced *Ptf1a*-expressing progenitors and analyzed pancreas development and function in mice.

RESULTS—Reduced *Ptf1a* dosage resulted in pancreatic hypoplasia and glucose intolerance with insufficient insulin secretion in a dosage-dependent manner. In hypomorphic mutant mice, pancreatic bud size was small and substantial proportions of pancreatic progenitors were misspecified to the common bile duct and duodenal cells. Growth with branching morphogenesis and subsequent exocrine cytodifferentiation was reduced and delayed. Total β-cell number was decreased, proportion of non-β islet cells was increased, and α-cells were abnormally intermingled with β-cells. Interestingly, *Pdx1* expression was decreased in early pancreatic progenitors but elevated to normal level at the mid-to-late stages of pancreatogenesis.

CONCLUSIONS—The dosage of *Ptf1a* is crucial for pancreas specification, growth, total β-cell number, islet morphogenesis, and endocrine function. Some neonatal diabetes may be caused by mutation or single nucleotide polymorphisms in the *Ptf1a* gene that reduce gene expression levels. *Diabetes* **57:2421–2431, 2008**

Spatiotemporally regulated expression of transcription factors is important for cell fate specification and organogenesis. It is becoming recognized that the absolute level of a specific transcription factor is also an important component for cell fate specification and differentiation, e.g., myogenin for skeletal muscle formation (1) and Sox2 for retinal progenitor cell differentiation and for the patterning and differentiation of anterior foregut endoderm (2,3). In pancreatogenesis, reduced dosage of *Pdx1* by deleting promoter elements of *Pdx1* causes a block in ventral pancreas specification and impaired dorsal pancreas development, resulting in glucose intolerance (4).

Ptf1a (PTF1-p48), a bHLH transcription factor, is indispensable for the formation of the exocrine pancreas and the correct spatial organization of the endocrine pancreas in mice (5). Originally, *Ptf1a* was reported as a transcriptional regulator for acinar cell–specific genes such as elastase 1 and amylase (6,7). Using Cre-mediated lineage tracing, we previously showed that all pancreatic exocrine cells and most endocrine cells derive from *Ptf1a*-expressing progenitors. Furthermore, by combining gene knockout and lineage tracing, we showed that *Ptf1a*-inactivated cells revert to an intestinal cell fate, demonstrating its function as a switch between pancreatic and intestinal cell fates (8). Supporting this notion, we and other groups recently demonstrated that ectopic expression of *Ptf1a* in the *Pdx1*-expressing undifferentiated endoderm results in a pancreatic cell fate and induces the full-scale pancreatic developmental program in mice and *Xenopus* (9–11). Very recently, it was shown that *Ptf1a* is one marker of early pancreatic multipotent progenitor cells located in the tips of the developing pancreatic epithelial tree (12). *Ptf1a* is not essential for pancreatic endocrine differentiation (5,8), and *Ptf1a* is not expressed in mature pancreatic endocrine cells (6). Nevertheless, in humans, nonsense mutations in *Ptf1a* were recently identified as a cause of permanent neonatal diabetes associated with pancreatic agenesis (13). The death of *Ptf1a*-null mice soon after birth has not allowed further insight into the pathogenesis of the disease; therefore, it is still unclear how much pancreatic endocrine function is dependent on *Ptf1a* in mammals. Moreover, there is no information about gene-dosage effect of *Ptf1a* on pancreas development and function in mice.

In the present study, we used a combination of hypomorphic and null alleles of *Ptf1a* and a Cre-mediated lineage-tracing approach to show that reduced dosage of *Ptf1a* results in pancreatic hypoplasia and glucose intolerance in mice. We provide evidence that there is a threshold of *Ptf1a* dosage by which pancreatic progenitor

cells proceed along the normal developmental pathway; they otherwise are misspecified to other organs (common bile duct [CBD]/duodenum) and cannot adequately expand in number. We also show defects in endocrine pancreas development (total β-cell number, ratios of endocrine cell types, and islet architecture) in *Ptf1a* hypomorphic mutant mice.

RESEARCH DESIGN AND METHODS

$Ptf1a^{cre/+}$ (8), $Ptf1a^{cbll/+}$ (14), and *ROSA26r* mice (15) were crossed in the C57BL/6 background and interbred to produce $Ptf1a^{cre/+}$;*ROSA26r*, $Ptf1a^{cre/cbll}$; *ROSA26r*, $Ptf1a^{cre/cre}$;*ROSA26r*, and $Ptf1a^{cbll/cbll}$ mice. All animal experiments were performed in accordance with the guidelines for animal experiments of Kyoto University.

RNA isolation and quantitative real-time RT PCR. Pancreatic rudiments were dissected and submerged in RNA Later (Qiagen, Tokyo, Japan). Total RNA was extracted using an RNeasy Mini Kit (Qiagen). First-strand cDNA synthesis was performed using Superscript III first-strand synthesis systems (Invitrogen). Quantification of *Ptf1a* and *Pdx1* gene expression was performed by quantitative real-time RT-PCR using the 7300 Real-Time PCR System (Applied Biosystems). The *Ptf1a* and *Pdx1* probes were TaqMan Gene Expression Assay nos. Mm00479622_m1 and Mm00435565_m1 (Applied Biosystems), respectively. Data were normalized in relation to the expression of GAPDH.

Histology. Tissue processing, X-gal staining, and permeabilization were performed as described previously (8,9). The following primary antibodies were used: guinea pig anti-insulin (DAKO), rabbit anti-amylase (Sigma-Aldrich), rabbit anti-glucagon (DAKO), rabbit anti-somatostatin (DAKO), rabbit anti-pancreatic polypeptide (DAKO), goat anti-*Pdx1*, goat anti-glut2 (Santa Cruz Biotechnology), mouse anti-cytokeratin (DAKO), and rabbit anti-phosphorylated histone H3 (Upstate). The immunofluorescent secondary antibodies were Cy3-conjugated antibody to guinea pig IgG (Cy3-conjugated antibody to rabbit IgG; Chemicon), Alexa Fluor 488-conjugated antibody to rabbit IgG (Molecular Probes), Alexa Fluor 488-conjugated antibody to mouse IgG (Molecular Probes), and Alexa Fluor 488-conjugated antibody to goat IgG (Molecular Probes). Transferase-mediated dUTP nick-end labeling (TUNEL) assays were performed using the DeadEnd Fluorometric TUNEL system (Promega). Images were visualized using a Zeiss Axioskop 2 microscope. Quantification of total β-cell number was performed by serially sectioning the entire pancreas followed by staining and counting every 10th section for embryonic day (e)14.5 embryos or every 20th section for e18.5 embryos ($n = 3$) in each genotype. The ratios of endocrine cell types were calculated from eight randomly chosen sections costained with hormones per animal ($n = 3$) in each genotype. Homogenized stool samples were centrifuged, and the supernatant was stained with Oil Red O solution (Sigma).

Glucose tolerance test and enzyme-linked immunosorbent assay. Glucose tolerance tests were performed by injecting D-glucose (2 mg/kg i.p.) after overnight fasting. For measurements of serum insulin, D-glucose (2 mg/g body wt i.p.) was injected and 15 min later blood was collected into tubes containing aprotinin (100 KIE/ml blood; Wako) and centrifuged to obtain serum. Plasma insulin levels were measured using the Mouse Insulin ELISA kit (u-type) (Shibayagi, Gunma, Japan).

Statistical analyses. Data are presented as mean ± SE. Data were subjected to unpaired t test or one-way nonrepeated measurements ANOVA with Bonferonni tests. $P < 0.05$ was considered significant.

RESULTS

Reduction of *Ptf1a* dosage resulted in small body size and pancreatic hypoplasia. A hypomorphic allele of *Ptf1a* ($Ptf1a^{cbll}$) has a 313-kb genomic deletion located 60 kb downstream of the *Ptf1a* locus, but the *Ptf1a* locus itself is intact (14). The $Ptf1a^{cre}$ allele is null through the replacement of the *Ptf1a* protein-coding region with that of a nuclearly targeted Cre recombinase (8). We used quantitative real-time RT-PCR to evaluate the expression level of *Ptf1a* in pancreata from $Ptf1a^{cre/+}$, homozygous $Ptf1a^{cbll/cbll}$, and compound trans-heterozygotes of $Ptf1a^{cre}$ and $Ptf1a^{cbll}$ ($Ptf1a^{cre/cbll}$) compared with that in wild-type mice at two stages: e12.5, when *Ptf1a* is expressed in the multipotent progenitor phase of pancreas development (12), and postnatal day 1 (P1), when *Ptf1a* is expressed in exocrine cells in pancreas. *Ptf1a* RNA levels in pancreatic

rudiments from $Ptf1a^{cre/+}$, $Ptf1a^{cbll/cbll}$, and $Ptf1a^{cre/cbll}$ mice were substantially reduced to 55 ± 8, 32 ± 10, and 14 ± 4%, respectively, compared with wild-type mice at e12.5, and they were reduced to 60 ± 7, 48 ± 4, and 30 ± 6%, respectively, at P1 (Fig. 1A).

Hypomorphic $Ptf1a^{cre/cbll}$ and $Ptf1a^{cbll/cbll}$ mice were born at the expected Mendelian ratio. $Ptf1a^{cre/cbll}$ mice appeared small and dehydrated at birth. Some $Ptf1a^{cre/cbll}$ mice survived to P30 (the longest survival up to P45), but the rest died before ~P14. On the other hand, $Ptf1a^{cre/+}$, $Ptf1a^{cbll/cbll}$, and wild-type mice were almost indistinguishable from each other at birth and were viable. As shown in Fig. 1B–D, postnatal growth retardation and small body size persisted into the weaning stage in $Ptf1a^{cre/cbll}$ and $Ptf1a^{cbll/cbll}$ mice. We crossed $Ptf1a^{cre/+}$ and $Ptf1a^{cre/cbll}$ with $Gt(ROSA)26Sor^{tm1Sor}$ (*R26r*) mice, which carry a floxed *lacZ* gene driven by cell type–independent *ROSA* promoter (15), enabling us to trace the fate of all *Ptf1a*-expressing cells and their progeny (8). Macroscopically, the pancreas of hypomorphic $Ptf1a^{cre/cbll}$;*R26r* mice was dramatically smaller than that of $Ptf1a^{cre/+}$;*R26r* mice at birth (data not shown), at P7, and at P30, and $Ptf1a^{cbll/cbll}$ mice exhibited moderate pancreatic hypoplasia (Fig. 1E–J).

Cell fate conversion of pancreatic precursors into the CBD and duodenal cells in $Ptf1a^{cre/cbll}$;*R26r* mice. Pancreas development can be divided into four phases in mice: The first phase is the specification and formation of dorsal and ventral pancreatic buds from foregut endoderm (specification). During the second phase, extensive proliferation and branching of the pancreatic epithelium occur (branching morphogenesis). The third phase involves differentiation of large numbers of endocrine, exocrine, and duct cell lineages (cytodifferentiation). The fourth phase consists of maturation of the islet architecture and function in the postnatal period (islet morphogenesis). Developmentally, as shown in Fig. 2A–H, pancreas was small from the beginning of pancreatic bud formation at e10.5 in $Ptf1a^{cre/cbll}$;*R26r* mice compared with $Ptf1a^{cre/+}$;*R26r* littermates, and this size difference became more apparent as development proceeded.

In our previous study, lineage-labeled β-galactosidase (β-gal)-positive cells were observed in the duodenum in both the dorsal and ventral regions in *Ptf1a*-null ($Ptf1a^{cre/cre}$; *R26r*) mice (8). A subset of β-gal–positive cells were found to protrude from the gut tube in the ventral region at e12.5, but the cell fate of these cells was not identified (8). In hypomorphic $Ptf1a^{cre/cbll}$;*R26r* mice, at the dorsal side, ectopic *Ptf1a* lineage-labeled areas were observed in the duodenum at P7, similar to $Ptf1a^{cre/cre}$;*R26r* mice at e17.5 (Fig. 1G and Fig. 2J). Notably, at the ventral side, not only the duodenum but also the CBD contained ectopic *Ptf1a* lineage-labeled cells in $Ptf1a^{cre/cbll}$;*R26r* at e17.5 and P7 (Fig. 2H and L) and in $Ptf1a^{cre/cre}$;*R26r* mice at e17.5 (Fig. 2K). Histologically, substantial proportions of *Ptf1a* lineage-labeled cells were misspecified and adopted a Cdx2 (16)-positive duodenal epithelial cell fate or cytokeratin-positive CBD epithelial cell fates including cells of the peribiliary glands (17) in $Ptf1a^{cre/cbll}$;*R26r* mice (Fig. 2M–Q). These results indicate that a threshold level of *Ptf1a* expression is required for the acquisition of a pancreatic cell fate in the primitive foregut endoderm and that reduction of *Ptf1a* dosage results in misspecification of pancreatic progenitors into the CBD and duodenum. Thus, together with reduced pancreatic bud size at early developmental stages, reduction of *Ptf1a* dosage results in a
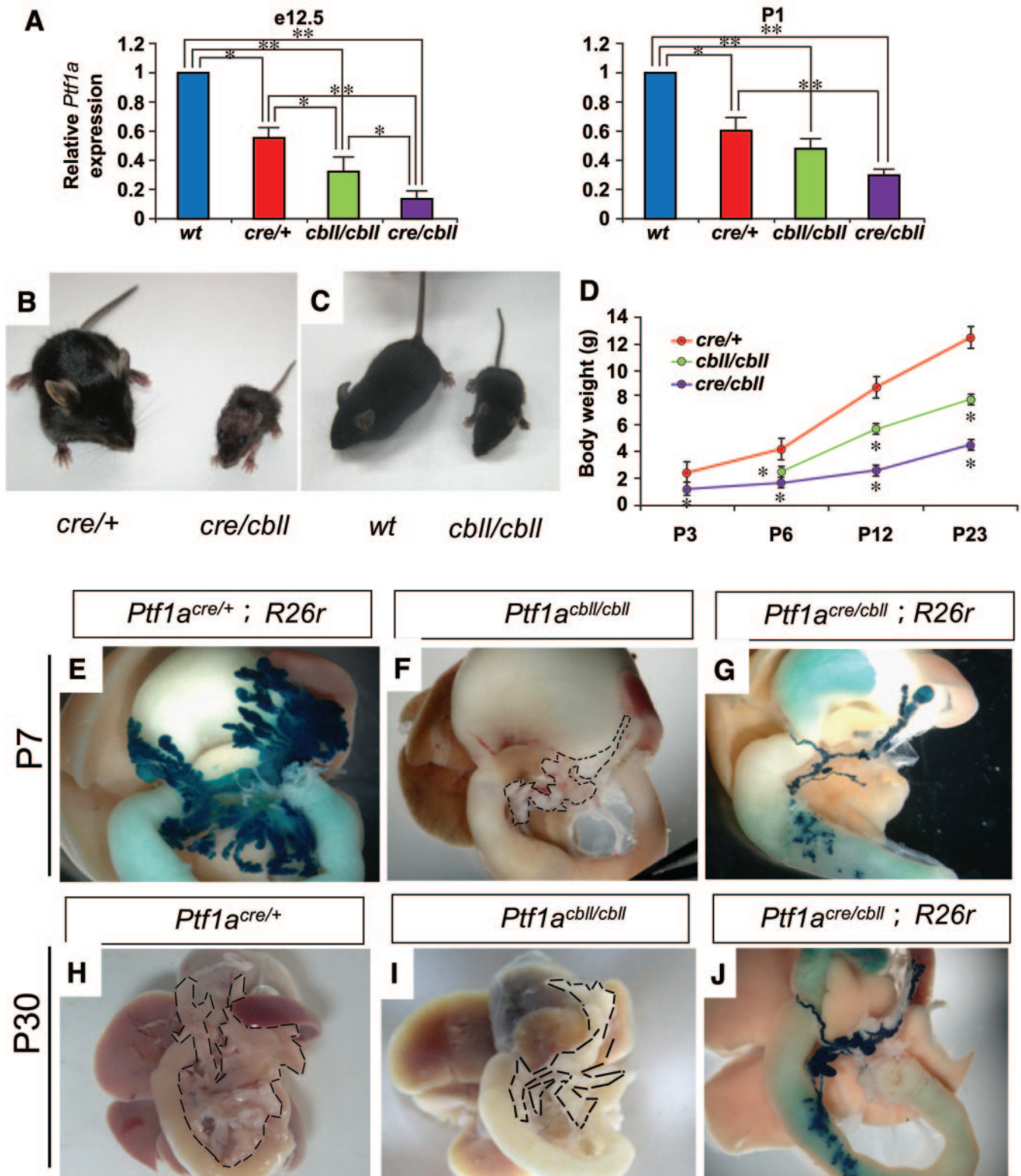
FIG. 1. Reduction of *Ptf1a* dosage results in small body size and pancreatic hypoplasia. *A*: Quantification of *Ptf1a* mRNA in pancreata by real-time RT-PCR. The relative expression levels of *Ptf1a* mRNA in pancreata from *Ptf1a* hypomorphic mice are shown compared with wild-type mice at e12.5 and P1. Data are expressed as means ± SE ($n = 4$). *$P < 0.05$, **$P < 0.01$. *B* and *C*: Gross appearance of *Ptf1a$^{cre/cbll}$* mice compared with *Ptf1a$^{cre/+}$* littermates (*B*) and *Ptf1a$^{cbll/cbll}$* mice compared with wild-type littermate (*C*) at P23. *D*: Body weights of *Ptf1a$^{cre/+}$*, *Ptf1a$^{cbll/cbll}$*, and *Ptf1a$^{cre/cbll}$* mice during postnatal periods. Data are expressed as means ± SE. *$P < 0.05$ compared with *Ptf1a$^{cre/+}$* mice. *E–G*: Macroscopic views of pancreata of *Ptf1a$^{cre/+}$;R26r* (*E*), *Ptf1a$^{cbll/cbll}$* (*F*), and *Ptf1a$^{cre/cbll}$;R26r* mice (*G*) at P7 stained with X-gal. Broken lines delineate pancreata in *F*, *H*, and *I*. At P30, pancreatic hypoplasia is observed in *Ptf1a$^{cbll/cbll}$* (*I*) and *Ptf1a$^{cre/cbll}$;R26r* mice (*J*) compared with *Ptf1a$^{cre/+}$* mice (*H*). (Please see http://dx.doi.org/10.2337/db07-1558 for a high-quality digital representation of this figure.)
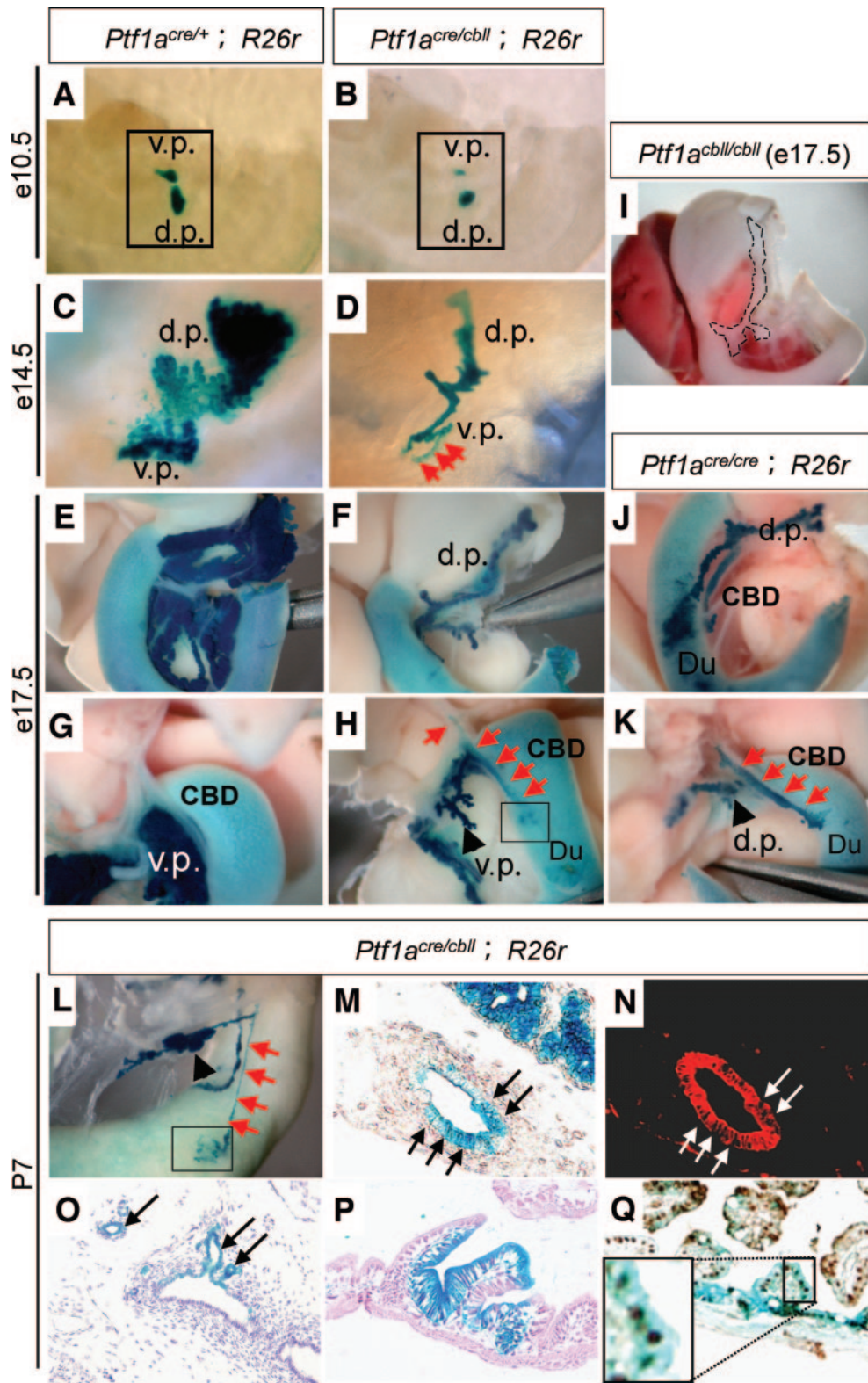
FIG. 2. Cell fate conversion of pancreatic precursors into the CBD and duodenal cells in hypomorphic *Ptf1a^cre/cbll* mice. *A–L*: Macroscopic views of pancreatic regions stained with X-gal. Hypomorphic pancreas is observed from the beginning of pancreatic bud formation at e10.5 (*B*) and becomes more apparent as development proceeds to e14.5 (*D*) and e17.5 (*F* and *H*) in *Ptf1a^cre/cbll*;*R26r* mice. Broken lines in (*I*) delineate moderate hypoplastic pancreas in *Ptf1a^cbll/cbll* mice at e17.5. Note that substantial proportions of the *Ptf1a* lineage-labeled cells are ectopically observed in the CBD (red arrows in *H*) and the duodenum (Du) (outlined boxes in *H* and *L*) in *Ptf1a^cre/cbll*;*R26r* mice at e17.5 (*H*) and P7 (*L*). Endogenous β-gal activity is observed in the duodenum as background. The cell fate conversion to the CBD is observed in *Ptf1a^cre/cbll*;*R26r* mice as early as e14.5 (red arrows in *D*). Ectopic *Ptf1a* lineage-labeled areas are also observed in the CBD and duodenum in *Ptf1a^cre/cre*;*R26r* mice at e17.5 (*J* and *K*). *M–Q*: Histological analyses of *Ptf1a^cre/cbll*;*R26r* mice at P7. Substantial proportions of *Ptf1a* lineage-labeled cells are misspecified and located to the CBD epithelium (arrows in *M* and *N* [*M* and *N* are the same sections]), including the peribiliary glands (arrows in *O*) and duodenal epithelial cells (*P*) stained with hematoxylin and eosin, which are positive for cytokeratin (red; arrow in *N*) and the intestinal marker Cdx2 (brown; *Q*), respectively, in *Ptf1a^cre/cbll*;*R26r* mice. (Please see http://dx.doi.org/10.2337/db07-1558 for a high-quality digital representation of this figure.)
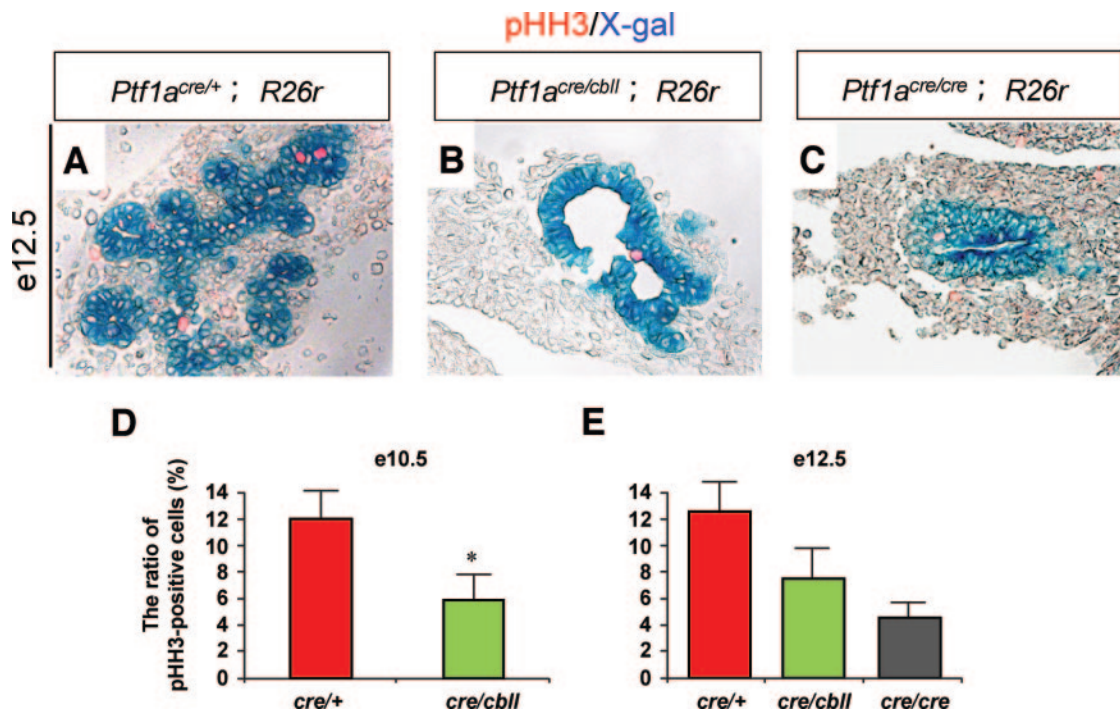
FIG. 3. Decreased proliferation of early pancreatic precursors in *Ptf1a* hypomorphic mutant mice. *A–C*: Sections of pancreata stained with X-gal and phosphorylated histone H3 (pHH3), a mitosis maker, at e12.5 (*A–C*). *D* and *E*: The ratios of pHH3-positive cells/*Ptf1a* lineage-labeled pancreatic epithelial cells at e10.5 (*D*) and e12.5 (*E*). Data are expressed as means ± SE ($n = 4$). *$P < 0.05$ compared with *Ptf1a$^{cre/+}$* mice. (Please see http://dx.doi.org/10.2337/db07-1558 for a high-quality digital representation of this figure.)

decrease in the final cell population that adopts a pancreatic cell fate.

Cell proliferation of the early pancreatic precursors is decreased in hypomorphic *Ptf1a$^{cre/cbll}$* mice. Next, we investigated whether reduction of *Ptf1a* dosage affects the growth of pancreatic precursor cells. Quantification revealed that significantly more pancreatic precursor cells are proliferating in *Ptf1a$^{cre/+}$* mice (12.0 ± 2.1% of the total *Ptf1a* lineage-labeled pancreatic epithelial cells) than in *Ptf1a$^{cre/cbll}$* mice (5.9 ± 1.9%) ($n = 4$, five to seven sections analyzed per embryo) at e10.5, as detected by the mitosis maker phosphorylated histone H3 (Fig. 3*D*). At e12.5, although the difference was not significant ($P = 0.071$), more pancreatic precursor cells were proliferating in *Ptf1a$^{cre/+}$* mice (6.3 ± 1.2%) than in *Ptf1a$^{cre/cbll}$* mice (3.8 ± 1.2%) and *Ptf1a$^{cre/cre}$* mice (2.3 ± 0.6%) (Fig. 3*A–C* and *E*). On the other hand, TUNEL staining revealed that apoptotic cells are only rarely observed in both *Ptf1a$^{cre/+}$* and hypomorphic mutant mice at e10.5 and e12.5 (data not shown), suggesting that apoptosis does not contribute to the hypomorphic pancreas of the mutants.

Delayed branching morphogenesis and reduced pancreatic exocrine differentiation with exocrine dysfunction in *Ptf1a* hypomorphic mice. As reported previously, *Ptf1a*-null mice completely lack exocrine cytodifferentiation (5,8). In *Ptf1a$^{cre/+}$;R26r* mice, extensive branching morphogenesis of the pancreatic epithelial tree was observed as early as e12.5, and amylase-positive cells were detected at e14.5 (Fig. 4*A.C*). In *Ptf1a$^{cre/cbll}$;R26r* mice, almost no branching morphogenesis of the pancreatic epithelial tree was seen, even at e14.5 (Fig. 4*B* and *E*). Exocrine cytodifferentiation was also markedly delayed and reduced (Fig. 4*H, K, N,* and *Q–T*). Amylase-positive cells began to appear at P1 in small areas in *Ptf1a$^{cre/cbll}$* mice, but they were morphologically immature in that the nucleus-to-cytoplasm ratio in *Ptf1a$^{cre/cbll}$* mice at P1 was as

large as that in *Ptf1a$^{cre/+}$* mice at e14.5 (Fig. 4*C* and *K*). At P7, pancreatic acinar structures were observed in restricted ventral regions, but the majority of the cells resembled immature duct-like epithelial structures that phenotypically corresponded to those at ~e14.5 in *Ptf1a$^{cre/+}$* mice (Fig. 4*N* and *Q*). In the adult stage, amylase-positive acinar structures were detected in the ventral pancreas and proximal dorsal pancreas, but the majority of dorsal pancreas was composed of immature duct-like epithelial cells that rarely expressed amylase (Fig. 4*R–T*). Persistent *Pdx1* expression was observed in the immature duct-like epithelial cells at P1, P7, and P30, while normal duct cells do not express *Pdx1* at these stages (Fig. 8*E–G* and *I* and data not shown). Thus, the reduced dosage of *Ptf1a* falls below the threshold required to elicit the proper pancreatic exocrine differentiation program, and many pancreatic duct-like epithelial cells appear to remain in an undifferentiated state until the adult stage. These results also indicate regional (ventral vs. dorsal and distal vs. proximal) differences in the exocrine differentiation program of the dorsal pancreas related to the *Ptf1a* dosage. *Ptf1a$^{cbll/cbll}$* mice showed intermediate delay in branching morphogenesis and exocrine cytodifferentiation during embryogenesis, but exocrine cytodifferentiation was fully restored by adulthood (Fig. 4*D, G, J, M,* and *P*). Actually, the body weights of *Ptf1a$^{cbll/cbll}$* mice were almost similar to those of wild-type mice by ~3 months of age. As expected from the histological findings, *Ptf1a$^{cre/cbll}$* mice showed exocrine pancreas dysfunction at P22, demonstrated by the abundant Oil red O–stained lipid droplets in stool smears (Fig. 4*U*). A small amount of lipid droplets was also observed in stool smears from *Ptf1a$^{cbll/cbll}$* mice, but it was very rare. Thus, we hypothesize that exocrine pancreas dysfunction is, at least in part, one of the causes of growth retardation as well as impaired metabolic homeostasis in *Ptf1a$^{cre/cbll}$* mice (see below).
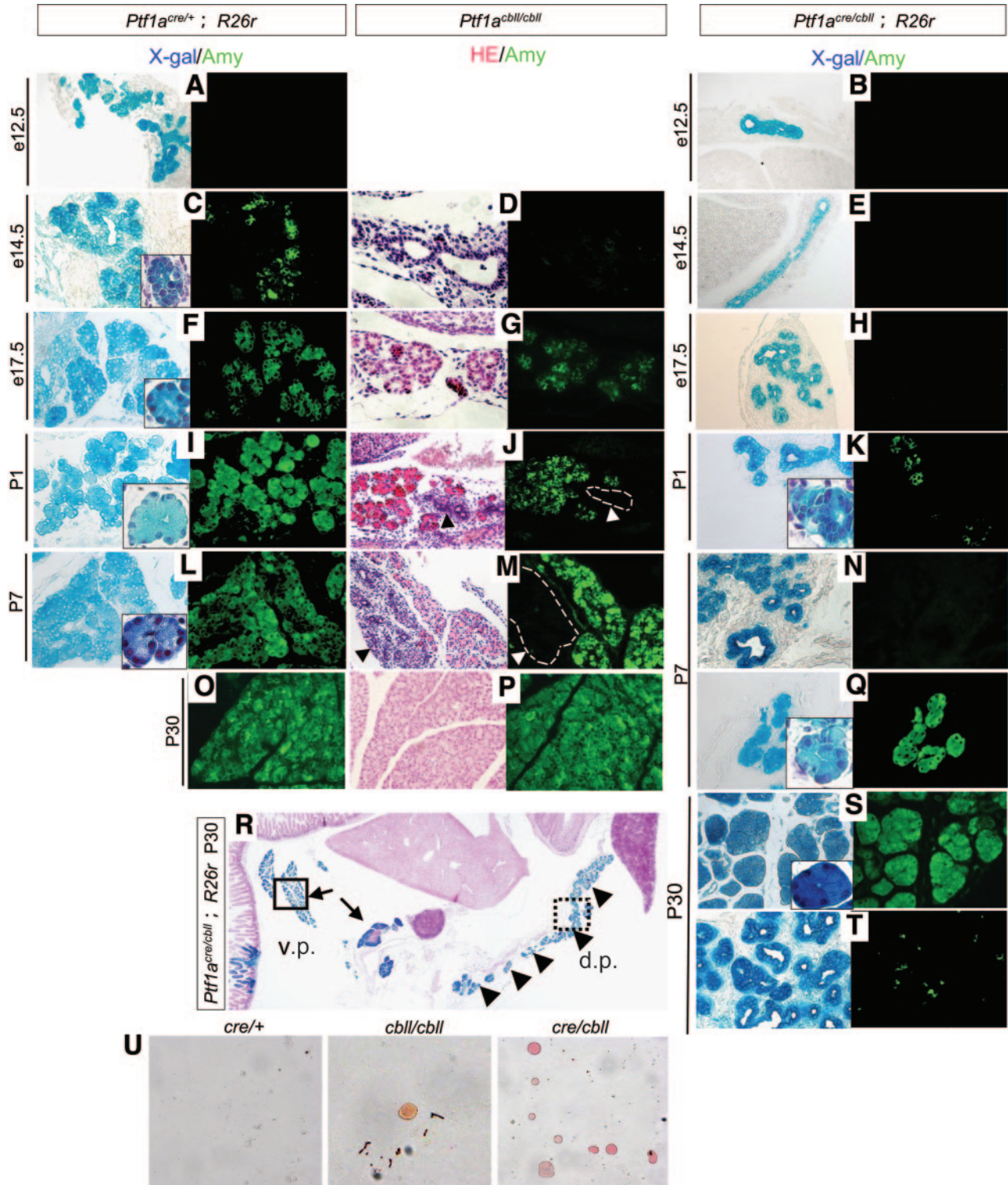
FIG. 4. Exocrine cytodifferentiation is reduced during development with delayed branching morphogenesis in hypomorphic mutant mice. *A–T*: Sections of pancreata stained with X-gal (blue) and amylase (Amy, green). (*Left panels* in *D, G, J, M, P,* and *R*: hematoxylin and eosin [HE] staining.) Extensive branching morphogenesis of the pancreatic epithelial tree is observed at both e12.5 and e14.5 in *Ptf1a^{cre/+};R26r* mice (*A* and *C*), whereas almost no branching morphogenesis is observed in *Ptf1a^{cre/cbll};R26r* mice at those stages (*B* and *E*). At e17.5, branching of the pancreatic epithelium could be observed in *Ptf1a^{cre/cbll};R26r* mice (*H*). At e14.5, amylase-positive cells are observed in *Ptf1a^{cre/+}* mice (*C*), whereas they are not seen at all in *Ptf1a^{cre/cbll}* (*E*) and *Ptf1a^{cbll/cbll}* mice (*D*). Amylase-positive cells are first apparent at P1 in *Ptf1a^{cre/cbll}* mice (*K*), but they are premature in that the nucleus-to-cytoplasm ratio in pancreatic exocrine cells of *Ptf1a^{cre/cbll}* mice at P1 is as large as that of *Ptf1a^{cre/+}* mice at e14.5 (outlined boxes in *K* and *C*). In some areas, normal pancreatic acinar structures are observed at P7 in *Ptf1a^{cre/cbll}* mice (*Q*), but the nucleus-to-cytoplasm ratio of the acinar cells in *Ptf1a^{cre/cbll}* mice at P7 is as large as that of *Ptf1a^{cre/+}* mice at e17.5 (outlined boxes in *Q* and *F*). At P30, in the ventral pancreas (v.p.) and the proximal dorsal pancreas (d.p.) in *Ptf1a^{cre/cbll}* mice, amylase-positive acinar structures are observed (arrows and outlined box in *R* and *S*), whereas, in their dorsal pancreas, the duct-like structures still exist (arrowheads and dashed-line box in *R*) and rarely express amylase (*T*). In *Ptf1a^{cbll/cbll}* mice, immature duct-like epithelial cells (arrowheads and dashed-lined boxes in *J* and *M*) are observed at P1 and P7, but acinar tissues are fully developed at P30 (*P*). *U*: Stool smears of *Ptf1a^{cre/+}*, *Ptf1a^{cbll/cbll}*, and *Ptf1a^{cre/cbll}* mice stained with Oil Red O. Large numbers of undigested lipid droplets are observed in stool smears of *Ptf1a^{cre/cbll}* mice, indicative of maldigestion. Very rarely, a small amount of lipid droplets is also observed in stool smears of *Ptf1a^{cbll/cbll}* mice. (Please see http://dx.doi.org/10.2337/db07-1558 for a high-quality digital representation of this figure.)
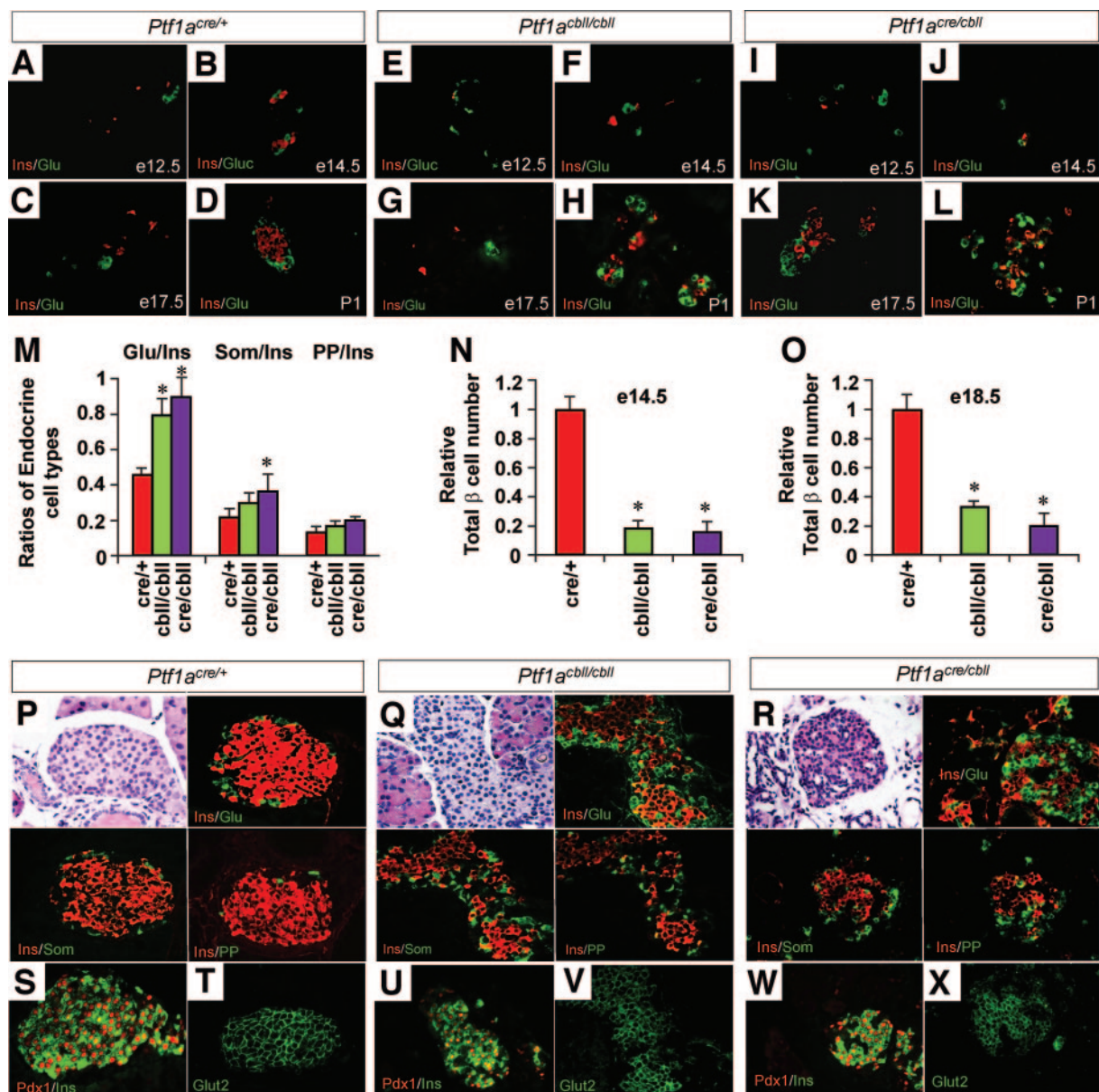
FIG. 5. Endocrine pancreas development in *Ptf1a* hypomorphic mutant mice. *A–L*: Sections of pancreata costained for insulin (red) and glucagon (green). Normal islet structures are observed in *Ptf1a*cre/+ mice at P1 (*D*), whereas they are not observed in *Ptf1a*cbll/cbll (*H*) and *Ptf1a*cre/cbll mice (*L*). *M*: Ratios of endocrine cell types at e18.5 in *Ptf1a*cre/+ (red bars), *Ptf1a*cbll/cbll (green bars), and *Ptf1a*cre/cbll mice (purple bars). *N* and *O*: Relative total β-cell number at e14.5 (*N*) and e18.5 (*O*) in each genotype. *P–R*: Representative sections of pancreatic islets colabeled for insulin (Ins, red) and glucagon (Glu, green), somatostatin (Som, green), or pancreatic polypeptide (PP, green) at P30. Note that pancreatic α-, ε-, and δ-cells are increased in number and α-cells are intermingled with β-cells in *Ptf1a*cbll/cbll and *Ptf1a*cre/cbll mice. *S–X*: Colabeling for *Pdx1* (red) and insulin (green) and staining for Glut2 (green) in islets. Pancreatic β-cells express *Pdx1* and Glut2 in all genotypes at P30, suggesting their maturation. Data are expressed as means ± SE (*n* = 3). *$P < 0.05$ compared with *Ptf1a*cre/+ mice. (Please see http://dx.doi.org/10.2337/db07-1558 for a high-quality digital representation of this figure.)

Abnormal islet formation with insufficient insulin secretion and glucose intolerance in *Ptf1a* hypomorphic mutants. During embryogenesis, the timing of pancreatic endocrine cytodifferentiation was indistinguishable between *Ptf1a*cre/+, *Ptf1a*cbll/cbll, and *Ptf1a*cre/cbll mice (Fig. 5*A–L*). However, analyses of endocrine cell types at e18.5 revealed that the ratio of α- to β-cells is significantly higher in *Ptf1a*cre/cbll and *Ptf1a*cbll/cbll mice and the ratio of δ- to β-cells is significantly higher in *Ptf1a*cre/cbll mice compared with *Ptf1a*cre/+ mice (*n* = 3) (Fig. 5*M*). Moreover, total number of β-cells was significantly lower in *Ptf1a*cre/cbll and *Ptf1a*cbll/cbll mice compared with *Ptf1a*cre/+ mice at both e14.5 and e18.5 in a *Ptf1a* dosage–dependent manner (*n* = 3) (Fig. 5*N* and *O*). At postnatal

stages (at P1 and at P30), islet architecture was disorganized in both *Ptf1a*cre/cbll and *Ptf1a*cbll/cbll mice (Fig. 5*D*, *H*, *L*, and *P-R*). The proportion of glucagon-producing cells was increased, and many of them were abnormally intermingled with islet β-cells (Fig. 5*P–R*). Pancreatic polypeptide– and somatostatin-expressing cells were normally localized in the periphery of islet but increased in number in both *Ptf1a*cbll/cbll and *Ptf1a*cre/cbll mice (Fig. 5*P–R*). Nuclear *Pdx1* and cell-membranous Glut2 expressions in individual β-cells were similar to those in wild-type mice at P30 (Fig. 5*S–X*), suggesting their maturation.

To assess pancreas endocrine function, mice (23- to 30-day-old: wild-type, *n* = 4; *Ptf1a*cre/+, *n* = 16; *Ptf1a*cbll/cbll,
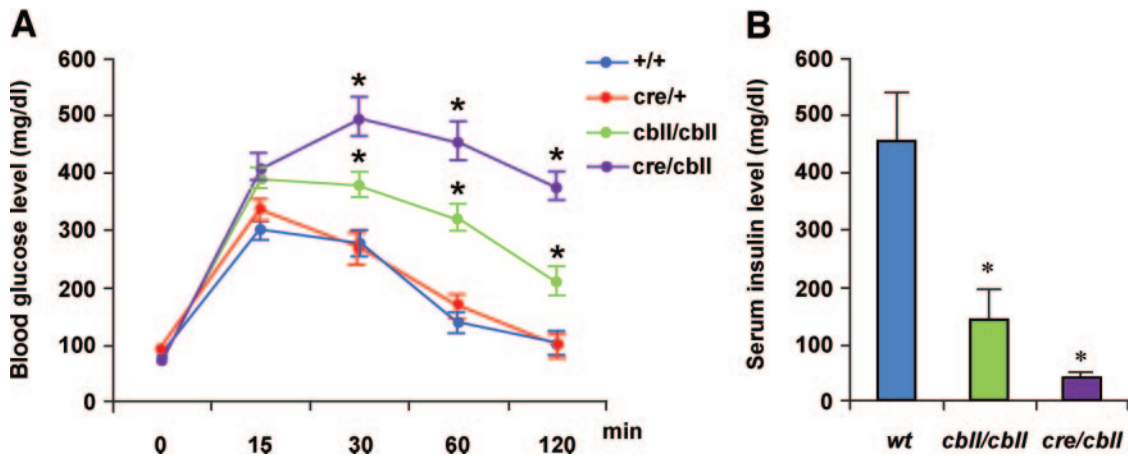
FIG. 6. Impaired glucose tolerance with insufficient insulin secretion in *Ptf1a* hypomorphic mutant mice. *A*: Blood glucose levels during intraperitoneal glucose tolerance test (data from 21- to 30-day-old wild-type, $n = 4$; *Ptf1a$^{cre/+}$*, $n = 16$; *Ptf1a$^{cbll/cbll}$*, $n = 33$; and *Ptf1a$^{cre/cbll}$* mice, $n = 6$). Note that glucose intolerance is observed in a *Ptf1a* dosage–dependent manner. *B*: Serum insulin levels 15 min after intraperitoneal glucose injection measured by enzyme-linked immunosorbent assay (data from 23- to 30-day-old wild-type, $n = 4$; *Ptf1a$^{cbll/cbll}$*, $n = 9$; and *Ptf1a$^{cre/cbll}$* mice, $n = 5$). Serum insulin levels are inappropriately lower in hypomorphic mutants compared with wild-type mice. Data are expressed as means ± SE. *$P < 0.05$ compared with wild-type mice.

$n = 33$; and *Ptf1a$^{cre/cbll}$*, $n = 6$) were subjected to intraperitoneal glucose tolerance tests. Strikingly, *Ptf1a$^{cre/cbll}$* mice showed dramatically elevated blood glucose levels 30 min after injection and remained hyperglycemic during the entire testing period compared with wild-type and *Ptf1a$^{cre/+}$* mice (Fig. 6*A*). *Ptf1a$^{cbll/cbll}$* mice exhibited mild glucose intolerance (Fig. 6*A*). Serum insulin levels at 15 min after intraperitoneal glucose injection were inappro-
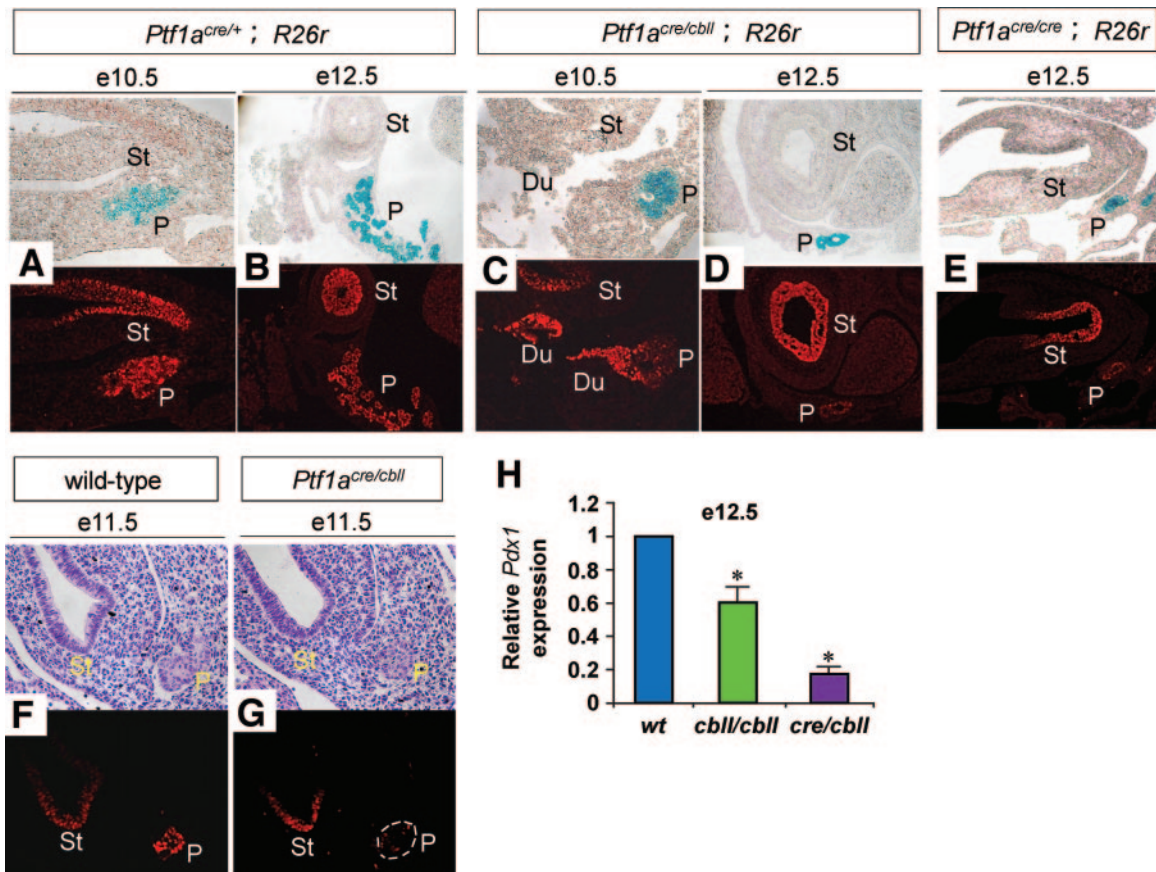

FIG. 7. *Pdx1* expression levels are reduced in early pancreatic precursors in *Ptf1a* hypomorphic mutant mice. *A–E*: Sections of pancreata stained with X-gal (blue) and *Pdx1* (red). *F* and *G*: Sections of pancreata stained for hematoxylin and eosin (*upper panels*) and Pdx1 protein (*lower panels*). Signal intensity is similar in the distal stomach epithelium, so that the *Pdx1* expression level in pancreatic precursors can be judged compared with it. Note that *Pdx1* expression is reduced in pancreatic precursors at e10.5, e11.5, and e12.5 in *Ptf1a$^{cre/cbll}$* mice compared with *Ptf1a$^{cre/+}$* and wild-type mice. *G*: Dashed line shows pancreatic epithelium. In *Ptf1a* null mice, *Pdx1* expression is also reduced at e12.5 (*E*). *H*: Quantification of *Pdx1* mRNA in pancreatic rudiments by real-time RT-PCR. The relative expression levels of *Pdx1* in pancreatic rudiments from *Ptf1a* hypomorphic mice are shown compared with wild-type mice at e12.5. Data are represented as means ± SE ($n = 4$). *$P < 0.05$ compared with wild-type mice. Du, duodenum; St, distal stomach; P, pancreas. (Please see http://dx.doi.org/10.2337/db07-1558 for a high-quality digital representation of this figure.)
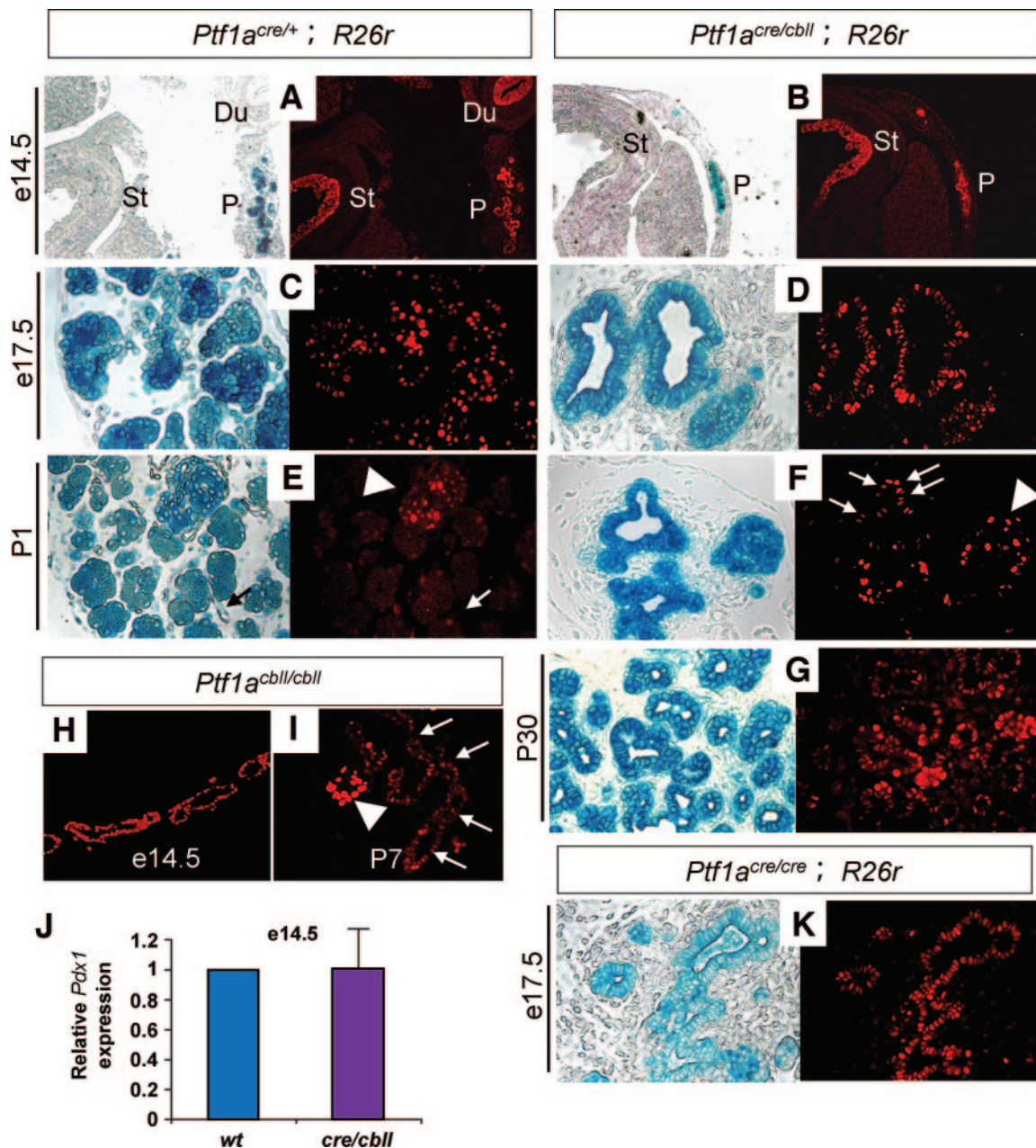
FIG. 8. *Pdx1* expression persists in the postnatal pancreatic duck-like epithelial cells in *Ptf1a* hypomorphic mutant mice. Sections of pancreata stained for X-gal (blue) and Pdx1 (red) (*A–G* and *K*) and stained for Pdx1 (*H* and *I*). The expression level of Pdx1 protein is similar among all genotypes at e14.5 and e17.5. At P1 and P30, strong *Pdx1* expression is observed in pancreatic β-cells in *Ptf1a$^{cre/+}$* mice (arrowhead in *E*), and its lower expression is maintained in pancreatic exocrine cells, whereas *Pdx1* expression is not observed in duct cells (arrows in *E*). Note that a moderate level of *Pdx1* expression persists in the pancreatic duck-like epithelial cells in *Ptf1a$^{cre/cbll}$* mice at P1 (arrows in *F*) and P30 (*G*) and in *Ptf1a$^{cbll/cbll}$* mice at P7 (arrows in *I*). The arrowhead in *F* shows strong *Pdx1* expression in β-cells in *Ptf1a$^{cre/cbll}$* mice. *J*: Quantification of *Pdx1* mRNA in pancreatic rudiments by real-time RT-PCR. The relative expression levels of *Pdx1* in pancreatic rudiments of *Ptf1a$^{cre/cbll}$* mice are shown compared with those of wild-type mice at e14.5. Data are expressed as means ± SE ($n = 4$). Du, duodenum; St, distal stomach; P, pancreas. (Please see http://dx.doi.org/10.2337/db07-1558 for a high-quality digital representation of this figure.)

priately low in *Ptf1a$^{cre/cbll}$* (39 ± 0.6 pg/ml, $n = 5$) and *Ptf1a$^{cbll/cbll}$* mice (142 ± 46 pg/ml, $n = 9$) compared with wild-type mice (453 ± 107 pg/ml, $n = 5$) (Fig. 6*B*).

Pdx1 expression is decreased in early pancreatic precursors in *Ptf1a$^{cre/cbll}$* mice. *Pdx1* is essential for pancreas organogenesis and mature pancreatic β-cell function in mice and humans (18–20). A recent study has shown that Ptf1a activates *Pdx1* expression in vitro and that endogenous Ptf1a binds the regulatory sequences of *Pdx1* in vivo (21,22). Consistent with these findings, *Pdx1* expression was substantially reduced in pancreatic precursor cells in *Ptf1a$^{cre/cbll}$* mice at e10.5, e11.5, and e12.5

and in *Ptf1a$^{cre/cre}$* mice at e12.5 compared with *Ptf1a$^{cre/+}$* or wild-type mice (Fig. 7*A–G*, cf. signal intensity in the distal stomach vs. dorsal pancreas). *Pdx1* RNA levels in pancreatic rudiments from *Ptf1a$^{cbll/cbll}$* and *Ptf1a$^{cre/cbll}$* mice at e12.5 were significantly decreased to 63 ± 2 and 17 ± 5%, respectively, compared with wild-type mice (Fig. 7*H*). Interestingly, *Pdx1* expression and *Pdx1* RNA levels in *Ptf1a* hypomorphic and null mutants were elevated and reached the same level as those in *Ptf1a$^{cre/+}$* and wild-type mice at e14.5 and 17.5 (Fig. 8*A–D*, *H*, *J*, and *K* and data not shown). Considering that *Ptf1a* dosage is still low at P1 in each mutant, other positive regulators of *Pdx1* would be

responsible for *Pdx1* reactivation at the mid-to-late stages of pancreatogenesis.

DISCUSSION

In the present study, combining hypomorphic and null alleles of *Ptf1a* with Cre-loxP–based lineage tracing, we have revealed dosage-dependent, crucial roles of *Ptf1a* in pancreatic development and function, including *1*) determination of pancreas size throughout embryogenesis until the weaning stage, *2*) cell fate determination of the pancreas versus CBD or duodenum in the developing foregut endoderm, *3*) growth with branching morphogenesis of the epithelial tree and exocrine cytodifferentiation, *4*) total β-cell number and balance of endocrine cell types, and *5*) islet morphogenesis and endocrine function in the postnatal period. These findings are implicated in possible pathogenesis of pancreatic hypoplasia and neonatal diabetes in humans.

The crucial role of *Ptf1a* dosage as a determinant of pancreatic size. We have observed dosage-dependent pancreatic hypoplasia in *Ptf1a* hypomorphic mutant mice. Accounting for hypoplastic pancreas, we have revealed that reduction of *Ptf1a* dosage results in a decrease of the final cell population that adopts a pancreatic cell fate. Furthermore, we have shown that subsequent growth of early pancreatic precursors is also reduced in *Ptf1a* hypomorphic mutants. Recently, it was reported that Pdx1^{+} Ptf1a^{+} cMyc[high] Cpa1^{+} multipotent progenitor cells are located in the tip of the branching pancreatic epithelial tree, while the trunk region of branches is composed of endocrine and duct cell precursors (12). In *Ptf1a* hypomorphic mutants, it is conceivable that reduced branching morphogenesis might result in the decrease in the number of "multipotent tip cells." In addition, consistent with the recent studies (21,22), we have demonstrated that *Ptf1a* dosage is crucial for the activation of *Pdx1* in early pancreatic progenitors in vivo. Considering that *Pdx1* inactivation results in early growth arrest (19) and that *Pdx1* positively regulates *Ptf1a* in the early pancreatic buds (4), it is concluded that Pdx1 and Ptf1a mutually activate each other in early pancreatic precursors, establishing the pancreatic domains in the primitive endoderm and promoting subsequent growth of pancreatic precursors. It is noteworthy that *Ptf1a* dosage is one of the "intrinsic" determinants of pancreatic size, which is relevant to a recent study suggesting that the pancreas size is determined by an intrinsic factor that is not amendable to growth compensation (23). It remains possible that substantial pancreatoneogenesis is still occurring at P1, although there is currently no evidence for multipotent progenitor cells that express *Ptf1a* at P1 and afterward.

The critical role of *Ptf1a* dosage in cell fate specification. It is interesting that the cells expressing reduced *Ptf1a* adopted different cell fates, including the CBD, duodenum, and pancreas in *Ptf1a*[cre/cbll] mice. Considering that the expression level of *Ptf1a* per cell appears to not be same in pancreatic buds at the early developmental stage (12,24), it is likely that the cells that express *Ptf1a* above a certain threshold level are specified to pancreas and those cells expressing *Ptf1a* below this level are specified to the CBD or duodenum. It is possible that the cells most likely to be misspecified are those at the duodenal junction, since they could potentially still be receiving some kind of gut fate-inducing signals that are stronger than in the more distal cells. On the other hand, it is still an open

question as to how pancreatic endocrine versus exocrine cell fate specification is determined. In the recent study, one striking observation is that Cpa1 becomes downregulated in the cleft region when the branching tips divide and Cpa1-expressing cells become incorporated into the trunk region (12). In this study, we have found that pancreatic exocrine cytodifferentiation is markedly delayed and reduced in *Ptf1a* hypomorphic mutants, whereas endocrine cytodifferentiation is less affected. Together with the report from Zhou et al. (12), our findings lead to an intriguing hypothesis that *Ptf1a* dosage might be a determinant of cell fate specification of pancreatic exocrine versus endocrine lineage: The pancreatic progenitor cells that express *Ptf1a* at a higher level are specified to exocrine lineage, whereas those that express *Ptf1a* at lower level are specified to endocrine lineage. It will be of considerable interest to test this hypothesis by chimeric mouse experiments using *Ptf1a* hypomorphic alleles.

The role of *Ptf1a* dosage in endocrine pancreas development and glucose homoeostasis. The present study shows that *Ptf1a* dosage affects total β-cell number and the balance of endocrine cell types as well as their relative spatial relationships in late-stage endocrine cell formation, although *Ptf1a* is not essential for endocrine cytodifferentiation. It has been suggested that the surrounding environment might be important for proper islet formation (5). In *Ptf1a* hypomorphic mutants, appropriate acinar tissues are not formed during embryognenesis and the neonatal period; therefore, it is possible that lack of production of the appropriate acinar tissue affects islet formation. Alternatively, it is possible that downregulation of *Pdx1* in early pancreatic multipotent progenitors affects a proportion of endocrine cell types in the mutants. Reducing *Pdx1* expression by deleting promoter elements of *Pdx1* gene results in disrupted proportion of each islet cell type and its distribution (4). Other mouse models of disorganized islet architecture, including transgenic overexpression of hepatocyte nuclear factor (HNF)-6 (25) and dominant-negative HNF-1α (26), also result in glucose intolerance. In all of these models, Glut2 is absent or largely reduced; therefore, β-cell dysfunction, including glucose sensing, is a main cause of diabetes. In *Ptf1a* hypomorphic mice, however, insulin-producing cells express normal amounts of Pdx1 and Glut2, suggesting their functional maturation. We consider the main cause of glucose intolerance to be the inadequate number of total β-cells. From the observations during embryonic stages, two mechanisms might be responsible: First, as a consequence of reduced *Ptf1a* expression, substantial proportion of foregut epithelial cells are misspecified to the duodenum and CBD, resulting in the reduction of the final cell population that adopts a pancreatic cell-fate. Second, reduced proliferation during early pancreatogenesis causes inadequate expansion of endocrine precursor pools in *Ptf1a* hypomorphic mutant mice. Supporting this notion, preliminary analyses showed that *Ngn3* expression in pancreatic rudiments are reduced in *Ptf1a* hypomorphic mutants ($50 \pm 13\%$ in *Ptf1a*[cre/cbll] mice and $50 \pm 6\%$ in *Ptf1a*[cbll/cbll] mice) compared with wild-type mice at e12.5 ($n = 3$), although the expression level of *Ngn3* per cell is unclear. Reduced *Pdx1* expression might affect Ngn3-expressing cell formation during early pancreatigenesis in *Ptf1a* hypomorphic mutants because loss of *Pdx1* results in no Ngn3-expressing cell formation in mice (27). At the same time, islet dysmorphology itself (disturbed ratio of each cell type and its localization) might be associated

with decreased function. Mixing of peripheral cell types with β-cells might disrupt the gap junctional or other coupling that is involved in an efficient insulin release (28).

Clinical implications for *Ptf1a* hypomorphic mutant mice. We have already reported that hypomorphic *Ptf1a*$^{cre/cbll}$ and *Ptf1a*$^{cbll/cbll}$ mice exhibit cerebellar agenesis similar to that of *Ptf1a*-null mice (14). The levels of *Ptf1a* transcripts in *Ptf1a*$^{cbll/cbll}$ embryos are dramatically reduced in the cerebellum (26.3-fold reduction), whereas they are more mildly affected in the hindbrain (4.5-fold reduction) and pancreas (3.1-fold reduction) (Fig. 1 and ref. 29). The precise mechanism that accounts for this difference is currently unknown; however, our previous report and current findings suggest that threshold levels to acquire specific cell fates differ among different organs. A nonsense mutation in *Ptf1a* has been recently identified as a cause of autosomal recessively inherited permanent neonatal diabetes associated with pancreatic and cerebellar agenesis in humans (13). Although hypomoprhic *Ptf1a* alleles have not been identified so far, our data predict a possible involvement of hypomorphic *Ptf1a* alleles in congenital pancreatic hypoplasia and diabetes in humans either by mutations in the *Ptf1a* coding region or deletions or single nucleotide polymorphisms in its regulatory sequence that are pivotal in pancreatic *Ptf1a* expression. In addition, our findings are also implicated in possible islet regeneration therapy for diabetes, since controlling gene dosage or levels/duration of gene expression might be one of the important factors for producing pancreatic β-cells in vitro.

ACKNOWLEDGMENTS

REFERENCES

1. Vivian JL, Gan L, Olson EN, Klein WH: A hypomorphic myogenin allele reveals distinct myogenin expression levels required for viability, skeletal muscle development, and sternum formation. *Dev Biol* 208:44–55, 1999
2. Taranova OV, Magness ST, Fagan BM, Wu Y, Surzenko N, Hutton SR, Pevny LH: SOX2 is a dose-dependent regulator of retinal neural progenitor competence. *Genes Dev* 20:1187–1202, 2006
3. Que J, Okubo T, Goldenring JR, Nam KT, Kurotani R, Morrisey EE, Taranova O, Pevny LH, Hogan BL: Multiple dose-dependent roles for Sox2 in the patterning and differentiation of anterior foregut endoderm. *Development* 134:2521–2531, 2007
4. Fujitani Y, Fujitani S, Boyer DF, Gannon M, Kawaguchi Y, Ray M, Shiota M, Stein RW, Magnuson MA, Wright CV: Targeted deletion of a cis-regulatory region reveals differential gene dosage requirements for Pdx1 in foregut organ differentiation and pancreas formation. *Genes Dev* 20:253–266, 2006
5. Krapp A, Knofler M, Ledermann B, Burki K, Berney C, Zoerkler N, Hagenbuchle O, Wellauer PK: The bHLH protein PTF1-p48 is essential for the formation of the exocrine and the correct spatial organization of the endocrine pancreas. *Genes Dev* 12:3752–3763, 1998
6. Krapp A, Knofler M, Frutiger S, Hughes GJ, Hagenbuchle O, Wellauer PK: The p48 DNA-binding subunit of transcription factor PTF1 is a new exocrine pancreas-specific basic helix-loop-helix protein. *Embo J* 15:4317–4329, 1996
7. Rose SD, Swift GH, Peyton MJ, Hammer RE, MacDonald RJ: The role of PTF1–P48 in pancreatic acinar gene expression. *J Biol Chem* 276:44018–44026, 2001
8. Kawaguchi Y, Cooper B, Gannon M, Ray M, MacDonald RJ, Wright CV: The role of the transcriptional regulator Ptf1a in converting intestinal to pancreatic progenitors. *Nat Genet* 32:128–134, 2002
9. Fukuda A, Kawaguchi Y, Furuyama K, Kodama S, Horiguchi M, Kuhara T, Koizumi M, Boyer DF, Fujimoto K, Doi R, Kageyama R, Wright CV, Chiba T: Ectopic pancreas formation in Hes1-knockout mice reveals plasticity of endodermal progenitors of the gut, bile duct, and pancreas. *J Clin Invest* 116:1484–1493, 2006
10. Afelik S, Chen Y, Pieler T: Combined ectopic expression of Pdx1 and Ptf1a/p48 results in the stable conversion of posterior endoderm into endocrine and exocrine pancreatic tissue. *Genes Dev* 20:1441–1446, 2006
11. Jarikji ZH, Vanamala S, Beck CW, Wright CV, Leach SD, Horb ME: Differential ability of Ptf1a and Ptf1a-VP16 to convert stomach, duodenum and liver to pancreas. *Dev Biol* 304:786–799, 2007
12. Zhou Q, Law AC, Rajagopal J, Anderson WJ, Gray PA, Melton DA: A multipotent progenitor domain guides pancreatic organogenesis. *Dev Cell* 13:103–114, 2007
13. Sellick GS, Barker KT, Stolte-Dijkstra I, Fleischmann C, Coleman RJ, Garrett C, Gloyn AL, Edghill EL, Hattersley AT, Wellauer PK, Goodwin G, Houlston RS: Mutations in PTF1A cause pancreatic and cerebellar agenesis. *Nat Genet* 36:1301–1305, 2004
14. Hoshino M, Nakamura S, Mori K, Kawauchi T, Terao M, Nishimura YV, Fukuda A, Fuse T, Matsuo N, Sone M, Watanabe M, Bito H, Terashima T, Wright CV, Kawaguchi Y, Nakao K, Nabeshima Y: Ptf1a, a bHLH transcriptional gene, defines GABAergic neuronal fates in cerebellum. *Neuron* 47:201–213, 2005
15. Soriano P: Generalized lacZ expression with the ROSA26 Cre reporter strain. *Nat Genet* 21:70–71, 1999
16. Silberg DG, Swain GP, Suh ER, Traber PG: Cdx1 and cdx2 expression during intestinal development. *Gastroenterology* 119:961–971, 2000
17. Fukuda A, Kawaguchi Y, Furuyama K, Kodama S, Kuhara T, Horiguchi M, Koizumi M, Fujimoto K, Doi R, Wright CV, Chiba T: Loss of the major duodenal papilla results in brown pigment biliary stone formation in pdx1 null mice. *Gastroenterology* 130:855–867, 2006
18. Jonsson J, Carlsson L, Edlund T, Edlund H: Insulin-promoter-factor 1 is required for pancreas development in mice. *Nature* 371:606–609, 1994
19. Offield MF, Jetton TL, Labosky PA, Ray M, Stein RW, Magnuson MA, Hogan BL, Wright CV: PDX-1 is required for pancreatic outgrowth and differentiation of the rostral duodenum. *Development* 122:983–995, 1996
20. Stoffers DA, Zinkin NT, Stanojevic V, Clarke WL, Habener JF: Pancreatic agenesis attributable to a single nucleotide deletion in the human IPF1 gene coding sequence. *Nat Genet* 15:106–110, 1997
21. Wiebe PO, Kormish JD, Roper VT, Fujitani Y, Alston NI, Zaret KS, Wright CV, Stein RW, Gannon M: Ptf1a binds to and activates area III, a highly conserved region of the Pdx1 promoter that mediates early pancreas-wide Pdx1 expression. *Mol Cell Biol* 27:4093–4104, 2007
22. Miyatsuka T, Matsuoka TA, Shiraiwa T, Yamamoto T, Kojima I, Kaneto H: Ptf1a and RBP-J cooperate in activating Pdx1 gene expression through binding to Area III. *Biochem Biophys Res Commun* 362:905–909, 2007
23. Stanger BZ, Tanaka AJ, Melton DA: Organ size is limited by the number of embryonic progenitor cells in the pancreas but not the liver. *Nature* 445:886–891, 2007
24. Chiang MK, Melton DA: Single-cell transcript analysis of pancreas development. *Dev Cell* 4:383–393, 2003
25. Gannon M, Ray MK, Van Zee K, Rausa F, Costa RH, Wright CV: Persistent expression of HNF6 in islet endocrine cells causes disrupted islet architecture and loss of beta cell function. *Development* 127:2883–2895, 2000
26. Yamagata K, Nammo T, Moriwaki M, Ihara A, Iizuka K, Yang Q, Satoh T, Li M, Uenaka R, Okita K, Iwahashi H, Zhu Q, Cao Y, Imagawa A, Tochino Y, Hanafusa T, Miyagawa J, Matsuzawa Y: Overexpression of dominant-negative mutant hepatocyte nuclear fctor-1α in pancreatic β-cells causes abnormal islet architecture with decreased expression of E-cadherin, reduced β-cell proliferation, and diabetes. *Diabetes* 51:114–123, 2002
27. Burlison JS, Long Q, Fujitani Y, Wright CV, Magnuson MA: Pdx-1 and Ptf1a concurrently determine fate specification of pancreatic multipotent progenitor cells. *Dev Biol* 316:74–86, 2008
28. Caton D, Calabrese A, Mas C, Serre-Beinier V, Wonkam A, Meda P: Beta-cell crosstalk: a further dimension in the stimulus-secretion coupling of glucose-induced insulin release. *Diabete Metab* 28:3S45–S53, 2002
29. Yamada M, Terao M, Terashima T, Fujiyama T, Kawaguchi Y, Nabeshima Y, Hoshino M: Origin of climbing fiber neurons and their developmental dependence on Ptf1a. *J Neurosci* 27:10924–10934, 2007